Inorganic Chemistry

Article

pubs.acs.org/IC

Metal–Organic Frameworks with Tb_4 Clusters as Nodes: Luminescent Detection of Chromium(VI) and Chemical Fixation of CO_2

Jie Dong, Hang Xu, Sheng-Li Hou, Zhi-Lei Wu, and Bin Zhao*

Department of Chemistry, Key Laboratory of Advanced Energy Material Chemistry, MOE, and Collaborative Innovation Center of Chemical Science and Engineering (Tianjin), Nankai University, Tianjin 300071, China

Supporting Information

ABSTRACT: Two multifunctional metal–organic frameworks based on cubane-like tetrahedron Tb_4 clusters as nodes have been synthesized and characterized. Compound **1** exhibits a 2D lanthanide–organic framework with Tb_4 clusters as nodes, and compound **2** possesses a 3D framework with Tb_4 clusters and Mn^{2+} as nodes. Interestingly, luminescent investigations on them reveal that the two compounds can act as recyclable luminescent probes for chromium(VI) anion species and the corresponding detection limit can reach 10^{-7} mol/L. Furthermore, **1** and **2** own efficient catalytic activity for the chemical fixation of CO_2 with epoxides under mild conditions. Importantly, they both can be recycled at least three times without compromising the activity.

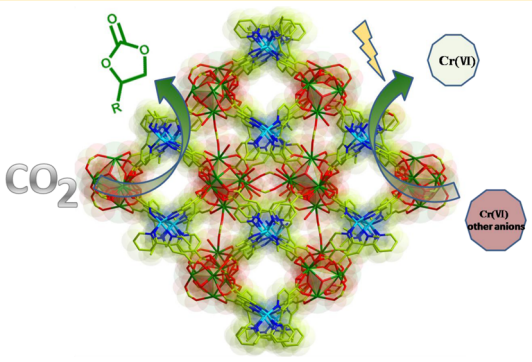

INTRODUCTION

As a promising class of porous materials, metal–organic frameworks (MOFs) have attracted immense attention because of not only their fascinating structures but also their potential applications in gas storage,[1] magnetism,[2] optical property,[3] chemical sensing,[4] catalysis,[5] etc. Among these applications, MOFs employed as chemical sensors have been extensively studied, and the hot issue of research mainly focused on the detection of anions,[6] cations,[7] and small organic molecules,[8] etc. However, a few studies have involved the detection of chromium(VI) anion species (CrO_4^{2-} or $Cr_2O_7^{2-}$), which are well-known toxic anions and pose a serious threat to human health and the environment, having been listed as a U.S. Environmental Protection Agency prior pollutant.[9] Nowadays, with the development of industry, more and more poisonous chromium(VI) species are discharged, and they were recognized or removed via conventional methods, such as ion exchange,[10] membrance separation,[11] photocatalytic degradation,[12] etc.[13] Nevertheless, these methods have the defects of poor regeneration and inferior chemical stability. Therefore, MOFs that have the incomparable advantages of high sensitivity, good regeneration, and excellent chemical stabilities as luminescent sensors to detect chromium(VI) anions are urgently needed to prevent chromium(VI) anions from endangering human health and the environment.

On the other hand, carbon dioxide (CO_2) chemistry has recently attracted much attention from the scientific community not only because the rapidly increasing atmospheric CO_2 levels are projected to have a detrimental consequence on the global climate but also because CO_2 is an inexpensive, nontoxic, renewable, and abundant C1 building block for organic synthesis.[14] Great effort has been devoted to developing methods or technologies to transform CO_2 into valuable raw materials.[15] One of the most promising technologies is the coupling reaction of CO_2 and epoxides to form cyclic carbonates,[16] which are important chemical intermediates and have been widely used in the synthesis of specialty fine chemicals and pharmaceuticals. Furthermore, the cycloaddition of CO_2 to an epoxide product with no byproducts is in accordance with green chemistry and atomic economy.[15c,e] With large-sized porosity and Lewis acidic sites, stable lanthanide-based MOFs are considered to be ideal candidates for CO_2 conversion with epoxides. As a kind of effective heterogeneous catalysis, MOF-based catalysts possess satisfactory circulation and separability,[17] which have good application prospects in industry.

With the above considerations in mind, two MOFs, $\{[Tb_4(BPDC)_4(\mu_3\text{-}OH)_4(H_2O)_8]\cdot 11H_2O\}_n$ (**1**) and $\{[Tb_4Mn(BPDC)_3(\mu_3\text{-}OH)_4(HCOO)_{1.5}(H_2O)_4]\cdot 2.5OH\cdot 8H_2O\}_n$ (**2**), based on Tb_4 clusters as nodes were obtained (H_2BPDC = 4,4′-dicarboxylate-2,2′-dipyridine anion). Compound **1** possesses a 2D framework with Tb_4 as nodes, while compound **2** is a 3D MOF based on $[Tb_4(OH)_4]^{8+}$ clusters and transition-metal Mn^{2+}, which both exhibit high thermal stability. Luminescence explorations reveal that compounds **1** and **2** can detect chromium(VI) anions with high sensitivity and recyclability and can serve as fluorescent probes for chromium(VI) anions. On the other hand, in terms of CO_2 conversion, compounds **1** and **2** can efficiently catalyze the cycloaddition reaction with CO_2 and epoxides under mild conditions;

Received: February 6, 2017

DOI: 10.1021/acs.inorgchem.7b00323
Inorg. Chem. XXXX, XXX, XXX−XXX

furthermore, these compounds can be reused at least three times without any obvious loss in catalytic activity.

EXPERIMENTAL SECTION

Preparation of $\{[Tb_4(BPDC)_4(\mu_3\text{-}OH)_4(H_2O)_8]\cdot 11H_2O\}_n$ (1). A mixture of $Tb(NO_3)_3\cdot 6H_2O$ (0.2 mmol, 90.6 mg), H_2BPDC (0.1 mmol, 24.4 mg), 100 μL of triethylamine, 4 mL of anhydrous alcohol, and 4 mL of distilled water was sealed in a 25 mL Teflon-lined stainless steel autoclave. The autoclave was heated at 200 °C for 72 h under autogenous presser and then cooled slowly to room temperature at a rate of 2 °C/h. Colorless flaky crystals were obtained and washed with distilled water. The yield was 65% [based on $Tb(NO_3)_3\cdot 6H_2O$]. Elem anal. Calcd for compound **1**: C, 28.65; H, 3.08; N, 5.57. Found: C, 29.09; H, 2.97; N, 5.31.

Preparation of $\{[Tb_4Mn(BPDC)_3(\mu_3\text{-}OH)_4(HCOO)_{1.5}(H_2O)_4]\cdot 2.5OH\cdot 8H_2O\}_n$ (2). Compound **2** was obtained in a manner similar to that of compound **1** except that $MnCl_2\cdot 4H_2O$ (0.05 mmol, 10 mg) was added. The yellow block crystals were washed with distilled water. The yield was 50% [based on $Tb(NO_3)_3\cdot 6H_2O$]. Elem anal. Calcd for compound **2**: C, 24.84; H, 2.76; N, 4.64. Found: C, 25.46; H, 2.36; N, 4.97.

RESULTS AND DISCUSSION

Structure Description of 1. Single-crystal X-ray diffraction (XRD) analysis reveals that compound **1** crystallizes in the tetragonal system with space group $I4_1/acd$, which shows a 2D layer structure. In the structure, the asymmetric unit contains a unique Tb^{3+} ion and one $BPDC^{2-}$ ligand, and the eight-coordinated Tb^{3+} ion is completed by three carboxylic oxygen atoms (O16, O19, and O20) of three $BPDC^{2-}$ ligands, two oxygen atoms (O21 and O23) of two water molecules, and three μ_3-oxygen atoms ($O2^a$, $O2^b$, and $O2^c$; Figure S1a). Four Tb^{3+} ions are bridged by μ_3-OH into a cubane-like tetranuclear cluster $[Tb_4(OH)_4]^{8+}$ (Figure 1a), which is further linked by eight $BPDC^{2-}$ ligands into a 2D framework (Figures 1b and S1e), possessing exposed nitrogen atom sites (Figure S1d).

Structure Description of 2. Considering the hollow distribution sites of nitrogen atoms in compound **1**, 0.05 mmol of $MnCl_2\cdot 4H_2O$ (10 mg) was added in the process of synthesis, and compound **2** was obtained. Structure analysis suggested that compound **2** crystallizes in the cubic system with space group $I2_13$. As illustrated in Figure S1b,c, the asymmetric unit has two crystallographically independent Tb^{3+} ions, in which the eight-coordinated Tb1 (Figure S1b) is surrounded by three carboxylic oxygen atoms (O4, O10, and O13), three μ_3-oxygen atoms (O5, $O9^a$, and $O9^b$), one oxygen atom (O2AA) from a coordinated water molecule, and one oxygen atom of a formic anion (O16), which is derived from decarboxylation of the H_2BPDC ligand, because aromatic compounds are more likely to decarboxylate under thermal insulation and alkaline conditions.[18] The seven-coordinated Tb2 (Figure S1c) is surrounded by three carboxylic oxygen atoms ($O11^a$, $O11^b$, and $O11^c$), three μ_3-oxygen atoms ($O9^a$, $O9^b$, and $O9^c$), and one oxygen atom (O14) from a coordinated water molecule. Four Tb^{3+} ions are bridged by four μ_3-OH into a tetranuclear cluster, $[Tb_4(OH)_4]^{8+}$ (Figure 1c), which shows a cubane-like structure. Furthermore, each $[Tb_4(OH)_4]^{8+}$ cluster is bridged with six $BPDC^{2-}$ ligands and three formate anions (Figure S1f), while the $[Tb_4(OH)_4]^{8+}$ cluster in **1** is linked with eight $BPDC^{2-}$ ligands. Additionally, every $[Tb_4(OH)_4]^{8+}$ cluster in **2** is bridged with three adjacent $[Tb_4(OH)_4]^{8+}$ clusters by three formate anions into a 3D framework, which possesses two kinds of different channels (Figure S2c,d) with diameters of 5 and 10.4 Å along the *c* direction. Six nitrogen atoms from three $BPDC^{2-}$ anions complete the six-coordinated environment of Mn^{2+} (Figure 1d), and the units $[Tb_4(OH)_4]^{8+}$ with Mn^{2+} are connected by $BPDC^{2-}$ into a 3D framework (Figure 1e). Along the *c* direction, **2** presents square channels with diameters ranging from 1.92 to 7.62 Å, and the potential total void volume of open channels in compound **2** is about 40.5%, as calculated by the *PLATON* program. Topological analysis showed that every $[Tb_4(OH)_4]^{8+}$ unit is bridged with six $[Mn(BPDC)_3]^{4-}$ units and three format anions to form an interesting 9-connected node, and every $[Mn(BPDC)_3]^{4-}$ unit is linked with six $[Tb_4(OH)_4]^{8+}$ units to form a 6-connected node. According to this simplification, the structure of compound **2** can be simplified as a 6,9-connected 3D framework with a topology symbol of sqc (Figure S2b).

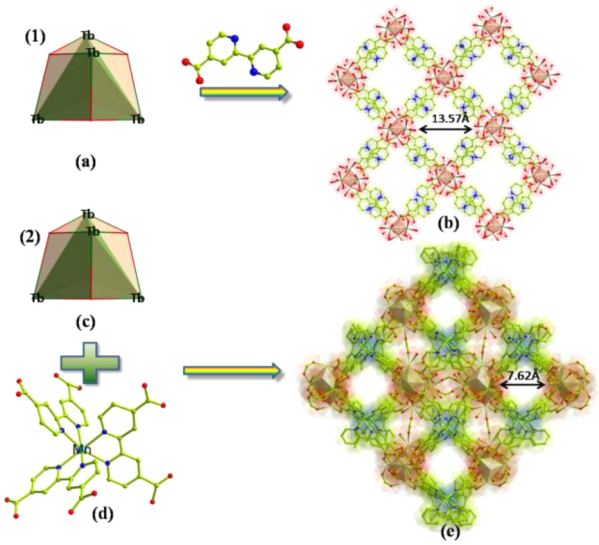

Figure 1. (a) $[Tb_4(OH)_4]^{8+}$ units of compound **1**. (b) 2D framework of **1** along the *c* direction. (c) $[Tb_4(OH)_4]^{8+}$ units of compound **2**. (d) $[Mn(BPDC)_3]^{4-}$ units of **2**. (e) 3D framework of **2** along the *c* direction. Hydrogen atoms and free water molecules are omitted for clarity.

Powder X-ray Diffraction (PXRD) Analysis and Thermogravimetric Analysis (TGA). The PXRD patterns of compounds **1** and **2** are recorded in Figure S3, and the PXRD patterns are almost in conformity with the simulated ones, indicating that compounds **1** and **2** are pure phases.

In order to study the thermal stability of the compounds, TGA was measured under a N_2 atmosphere, which are shown in Figure S4. The TGA curve of **1** shows that, from room temperature to 124 °C, a weight loss of 10.12% can be observed, which corresponds to the loss of free water molecules (calcd: 9.83%). Then, the curve shows a weight loss of 7.04% from 128 to 461 °C, corresponding to the loss of coordinated water molecules (calcd: 7.15%). Subsequently, compound **1** starts to decompose above 469 °C. Also, compound **2** shows high thermal stability. As shown in Figure S4, from room temperature to 122 °C, a weight loss of 8.42% can be observed in the TGA curve of **2**, which corresponds to the loss of free water molecules (calcd: 8.0%). With the temperature increasing, the curve shows a weight loss of 7.5% from 172 to 448 °C, corresponding to the loss of coordinated water molecules and formate anions (calcd: 7.62%). Then, compound **2** starts to decompose above 477 °C.

Luminescent Behaviors and Sensing Properties. The solid-state photoluminescence spectra of the free ligand

DOI: 10.1021/acs.inorgchem.7b00323
Inorg. Chem. XXXX, XXX, XXX−XXX

(H_2BPDC) and compounds **1** and **2** were measured under ambient conditions by excitation at 285 nm (Figure S7). Obviously, four characteristic emission peaks of Tb^{3+} are observed at 490, 544, 584, and 622 nm, which can be attributed to the transitions of $^5D_4 \rightarrow {}^7F_J$ (J = 6, 5, 4, and 3) from Tb^{3+} ions, respectively.[19] The strongest $^5D_4 \rightarrow {}^7F_5$ transition, which shows green-light emission, is assigned to the magnetic-dipole-induced transition.[4]

To explore the influence of different anions on the luminescence of **1**, 3 mg samples of **1** were dispersed in 2.7 mL of distilled water, forming a suspension solution by an ultrasonic method. Then 300 μL of a Na_mX (K_mX) solution (1×10^{-2} M; X = CH_3COO^-, IO_3^-, NO_3^-, BrO_3^-, Br^-, Cl^-, N_3^-, SO_4^{2-}, I^-, BF_4^-, ClO_4^-, SCN^-, $Cr_2O_7^{2-}$, CrO_4^{2-}, MnO_4^-) was slowly dropped into the above solutions to form a suspension of **1**-X in distilled water (1×10^{-3} M). With the perturbation of various anions, the resultant suspensions were monitored using a fluorescence spectrophotometer, and the corresponding luminescence curves still showed characteristic emission peaks (Figure S8) of Tb^{3+} ions. Then only the dominant emission peaks at 544 nm were recorded in Figure 2. Obviously, most

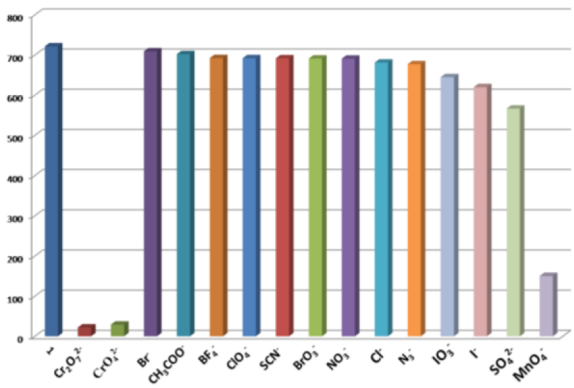

Figure 2. Ratio of $^5D_4 \rightarrow {}^7F_5$ transition intensities of **1** immersed in various Na_mX (K_mX) aqueous solutions (monitored at 544 nm).

anions display negligible influence on the emission or weaken the luminescence to some extent, while $Cr_2O_7^{2-}$ and CrO_4^{2-} exhibit a drastic quenching effect on the luminescence of **1**, which can be clearly observed, indicating that compound **1** can act as a promising chemical sensor of $Cr_2O_7^{2-}$ and CrO_4^{2-} among various anions. Because of the similar luminescent quenching phenomena of $Cr_2O_7^{2-}$ and CrO_4^{2-}, $Cr_2O_7^{2-}$ was chosen to serve as the representative in the study of luminescent behaviors and sensing properties.

In addition, to explore the detection limit of **1** as a $Cr_2O_7^{2-}$ probe, a series of suspensions of **1**-$Cr_2O_7^{2-}$ were prepared by dropping different concentrations of $Cr_2O_7^{2-}$ (10^{-7}–10^{-3} mol/L) in distilled water. The luminescence intensity of **1** gradually decreased with increasing concentration of $Cr_2O_7^{2-}$, and the decreased luminescence intensity still could be clearly observed when **1** was immersed in a 10^{-7} mol/L $Cr_2O_7^{2-}$ solution (Figure 3), indicating that the detection limit of **1** as a luminescent probe for detecting $Cr_2O_7^{2-}$ can reach 10^{-7} mol/L. To further explore the quenching effect of $Cr_2O_7^{2-}$ on the emission, a plot of the luminescence intensity versus $Cr_2O_7^{2-}$ concentration was made (Figure 3), which can be linearly fitted into the equation $I_0/I = 1.120 + K_{sv}[Cr_2O_7^{2-}]$ (I_0 and I represent the luminescence intensity of **1** before and after the addition of $Cr_2O_7^{2-}$ respectively; $[Cr_2O_7^{2-}]$ represents the

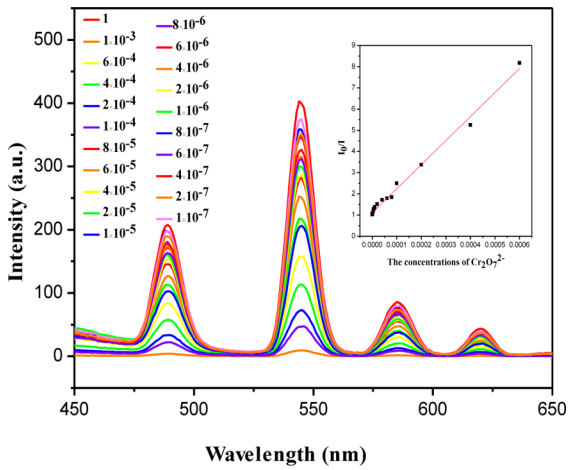

Figure 3. Emission spectra of **1** with different concentrations of $Cr_2O_7^{2-}$ ions and the luminescence intensity versus $Cr_2O_7^{2-}$ concentration plot.

concentration of $Cr_2O_7^{2-}$, and K_{sv} represents the quenching rate constant),[20] which is close to the Stern–Volmer equation $I_0/I = 1 + K_{sv}[Cr_2O_7^{2-}]$. The K_{sv} value is calculated to be 1.13×10^4 L/mol, revealing that $Cr_2O_7^{2-}$ displays a high quenching efficiency on the emission of compound **1**.

Because of the requirements of recyclability and economy for luminescent probes in practical applications, it is necessary to investigate the recycling performance of compound **1** as a $Cr_2O_7^{2-}$ luminescent probe. Herein, we attempted to simply immerse **1** in the water solution of 10^{-3} M $Cr_2O_7^{2-}$ ions for minutes to form **1**-$Cr_2O_7^{2-}$, and then **1**-$Cr_2O_7^{2-}$ was washed with water several times. As shown in Figures 4a and S12, the luminescence intensity and PXRD pattern of the recycled **1** are well consistent with the original results. Also, those experimental results agree with the original ones after being recycled five times, which indicates that compound **1** as a $Cr_2O_7^{2-}$ probe can be recycled with a fast and simple method.

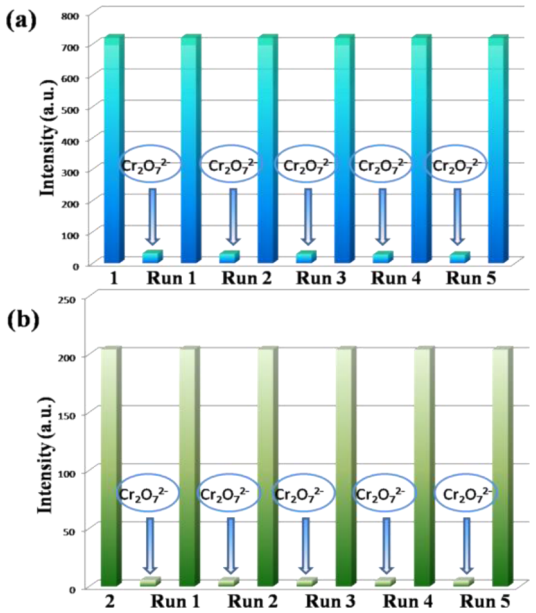

Figure 4. (a) Luminescent intensity (544 nm) of compound **1** after being recycled five times. (b) Luminescent intensity (544 nm) of compound **2** after being recycled five times.

DOI: 10.1021/acs.inorgchem.7b00323
Inorg. Chem. XXXX, XXX, XXX–XXX

Besides, the PXRD patterns of compound **1** immersed in different solvents were measured and remained well consistent with the simulated ones, indicating that the framework of **1** still remains stable (Figure S14). Additionally, in order to testify that there were no $Cr_2O_7^{2-}$ ions remaining in the framework after washing with water, the corresponding samples were measured by inductively coupled plasma (ICP) spectroscopy (Table S2), and the results show that there is only 0.012 ppm of Cr^{6+} residues in the framework of compound **1** after recycling five times, which indicates that the introduced $Cr_2O_7^{2-}$ ions have been removed completely.

Similar luminescent investigations on compound **2** were carried out, and the corresponding emission peaks (544 nm) were recorded. As shown in Figures S9 and S10, $Cr_2O_7^{2-}$ still exhibits a drastic quenching effect on the luminescence of **2**, and other anions have negligible effects on the emission. Moreover, the detection limit of **2** as a luminescent probe for detecting $Cr_2O_7^{2-}$ can also reach 10^{-7} mol/L. The quenching effect of $Cr_2O_7^{2-}$ on the emission was also explored. A plot of the luminescence intensity versus $Cr_2O_7^{2-}$ concentration was made (Figure S11), which could be linearly fitted into the equation $I_0/I = 1.003 + K_{sv}[Cr_2O_7^{2-}]$, close to the Stern−Volmer equation $I_0/I = 1 + K_{sv}[Cr_2O_7^{2-}]$, and the K_{sv} value is calculated to be 0.5×10^4 L/mol, revealing that $Cr_2O_7^{2-}$ displays a high quenching efficiency on the emission of compound **2**.

The recycling performance of compound **2** was also investigated. A similar experimental process was measured, and the corresponding results are recorded in Figures 4b and S13, indicating that compound **2** as a luminescent probe of $Cr_2O_7^{2-}$ can be recycled at least five times, with negligible loss in the luminescent response and PXRD well consistent with the original results. Meanwhile, the corresponding ICP (Table S2) reveals that the recycled samples do not contain $Cr_2O_7^{2-}$, and the recovered luminescence is attributed to the absence of $Cr_2O_7^{2-}$.

Then, the possible mechanism is discussed. First, well-matched PXRD results suggest that the frameworks are still intact after the introduction of $Cr_2O_7^{2-}$, proving that luminescence quenching is not caused by collapse of the framework. Second, from the UV−vis adsorption spectra of a $K_2Cr_2O_7$ aqueous solution (Figure S15) emerge strong absorption bands in the ranges of 230−312 and 312−500 nm, and the excitation wavelength of **1** and **2** is 285 nm, which indicates that a $Cr_2O_7^{2-}$ solution can significantly absorb the energy of the excitation wavelength, resulting in the luminescence quenching of **1** and **2**. Third, the concentration of $Cr_2O_7^{2-}$ and the luminescent intensity can be well fitted into the Stern−Volmer equation, indicating that the quenching process can be attributed to the dynamic process mechanism. That is to say, the adsorption of $Cr_2O_7^{2-}$ in the UV−vis region, as well as the collision interaction between structures and free $Cr_2O_7^{2-}$ anions, consumes the energy and reduces the luminescent intensity.

Catalytic Properties. Lanthanide metals are oxyphilic, and many of their compounds possess Lewis acidity. Considering the potential Lewis acidity of the two compounds, their catalytic capacities were explored, and here the transformation of CO_2 with epoxides as a model reaction was investigated. Styrene oxide was selected as a probe substrate to explore the optimized reaction conditions, and the corresponding results are recorded in Table 1. Under mild temperature (60 °C) and pressure (0.1 MPa), the reaction was conducted using 2.5 mol % cocatalyst tetrabutylammonium bromide (TBAB) and 2 mol % compound **1** or compound **2** (based on Tb_4 clusters), without solvent. The desired product 4-phenyl-1,3-dioxolan-2-one was obtained after 12 h, and the yield could reach 78% and 95%, respectively (entries 1b and 1c in Table 1). In contrast, the value was only 42% (entry 1a in Table 1) under 2.5 mol % TBAB without compound **1** or **2**, suggesting that these compounds play important roles in the reaction.

Table 1. Cycloaddition Reaction of CO_2 with Styrene Oxide under Various Conditions[a]

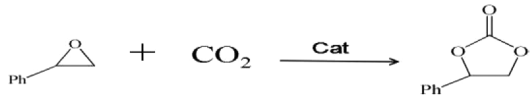

entry	catalyst	TBAB(mol %)	T (°C)	t (h)	yield (%)[b]
1a	0	2.5	60	12	42
1b	1	2.5	60	12	78
1c	2	2.5	60	12	95
2a	1	0	60	12	<1
2b	2	0	60	12	<1

[a]Reaction conditions: styrene oxide (240.3 mg, 2.0 mmol), solvent-free, catalysts **1** (25 mg, about 2 mol %, based on Tb_4 clusters) and **2** (22 mg, about 2 mol %, based on Tb_4 clusters), CO_2 (0.1 MPa), TBAB (17 mg, 2.5 mol %). [b]Determined by ^{1}H NMR spectroscopy using 1,3,5-trimethoxybenzene as an internal standard.

To further investigate the catalytic generality of compounds, various typical epoxide substrates were examined for the cycloaddition reaction. As showed in Table 2, substrates with electron-withdrawing groups generally had better yields. For example, the cycloaddition reactions of CO_2 with epichlorohydrin (entry 2) was effectively catalyzed in high yields (85% and 99%). When glycidyl phenyl ether (entry 3) and benzyl glycidyl ether (entry 4) were used, the desired products were generated with excellent yields (87% and 99%; 64% and 70%). The results can be explained by the fact that the electron-withdrawing substituents facilitate nucleophilic attack during the ring opening of the epoxide. However, the aliphatic hydrocarbon epoxide (entry 5), 1,2-epoxy-2-methylpropane (entry 6), and propylene oxide and 1,2-epoxyoctane (entry 7) were converted to the corresponding cyclic carbonate with low yield. In addition, compound **2** has a little higher catalytic efficiency than compound **1**, possibly due to the different CO_2 adsorption capacities (CO_2 adsorption/desorption of compound **2**, as shown in Figure S16, while CO_2 adsorption/desorption of compound **1** was not detected out), or the synergistic effect of Mn^{2+} in compound **2**.[21]

Additionally, as stable heterogeneous catalysts, the compounds could be separated from the reaction mixture through centrifugation and filtration. The recycle performances of compounds **1** and **2** were measured, and the corresponding results were recorded (Figure 5). ICP analysis (Table S2) of the reaction mixture filtrate reveals only 0.012 and 0.018 ppm of leakage from the robust frameworks, confirming the heterogeneous nature of the reaction. It is noted that the excellent catalytic activity of the two compounds still can be observed after the compounds were employed three times, and the robust frameworks of catalysts still remained intact, which is confirmed by PXRD investigations (Figures S12 and S13).

On the basis of the reported mechanism of the cycloaddition of CO_2 and epoxides, a tentative mechanism is discussed. Frameworks **1** and **2** with porous channels can enrich CO_2 and the substrate, then epoxides are activated by the Tb^{3+} sites in

DOI: 10.1021/acs.inorgchem.7b00323
Inorg. Chem. XXXX, XXX, XXX−XXX

Table 2. Cycloaddition Reaction of CO_2 with Various Substrates[a]

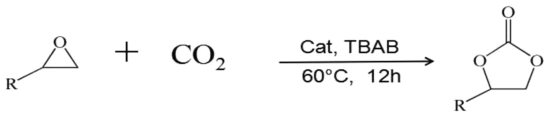

Entry	Subs	Prod	Yield(%)[b]
1a	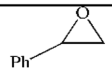		78
1b			95
2a	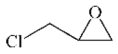	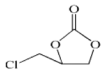	85
2b			>99
3a	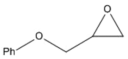	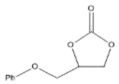	87
3b			>99
4a	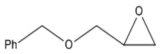	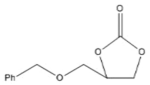	64
4b			70
5a			12
5b			20
6a			34
6b			40
7a	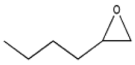	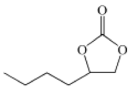	31
7b			42

[a]Reaction conditions: epoxides (2.0 mmol), solvent-free, catalysts **1** and **2** (25 and 22 mg, respectively, about 2 mol %, based on Tb_4 clusters), CO_2 (0.1 MPa), 60 °C, TBAB (17 mg, 2.5 mol %). [b]Determined by ^1H NMR spectroscopy using 1,3,5-trimethoxybenzene as an internal standard. Letter a in the table represents catalyst **1**, and letter b represents catalyst **2**.

compounds and Br^- effectively promotes the ring opening of the epoxides. Then, CO_2 and the oxygen anion of the opened ring react to form an alkylcarbonate salt. Finally, the corresponding cyclic carbonates are obtained through ring closure (Figure S18).

CONCLUSION

In conclusion, two multifunctional MOFs, $\{[Tb_4(BPDC)_4(\mu_3\text{-}OH)_4(H_2O)_8]\cdot 11H_2O\}_n$ and $\{[Tb_4Mn(BPDC)_3(\mu_3\text{-}OH)_4(HCOO)_{1.5}(H_2O)_4]\cdot 2.5OH\cdot 8H_2O\}_n$, were synthesized and characterized. Characterization of the structures showed that compound **1** exhibits a 2D framework with Tb_4 clusters as nodes and compound **2** possesses a 3D framework with Tb_4 clusters and Mn^{2+} as nodes. Interestingly, they both possess the capacity to detect chromium(VI) anion species after being recycled, and the detection limits for both can reach 10^{-7} mol/L. Importantly, these multifunctional compounds are demonstrated as new types of effective heterogeneous catalysts to catalyze the cyclization reaction with epoxides and CO_2, and the recycling number can reach three times.

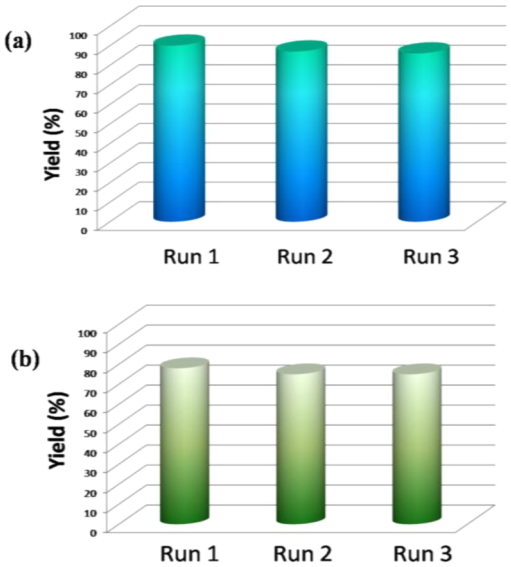

Figure 5. (a) Recycle tests of **1** for the cycloaddition reaction of CO_2 with styrene oxide. (b) Recycle tests of **2** for the cycloaddition reaction of CO_2 with styrene oxide.

ASSOCIATED CONTENT

Supporting Information

The Supporting Information is available free of charge on the ACS Publications website at DOI: 10.1021/acs.inorgchem.7b00323.

Synthesis, crystal data, IR, TGA, and PXRD (PDF)
X-ray crystallographic data in CIF format for **1** (CCDC 1520757) and **2** (CCDC 1520758) (CIF)

AUTHOR INFORMATION

Corresponding Author

*E-mail: zhaobin@nankai.edu.cn. Fax: (+86)-22-23502458.

ORCID

Bin Zhao: 0000-0001-9003-9731

Notes

The authors declare no competing financial interest.

ACKNOWLEDGMENTS

This work was supported by the NSFC (Grants 21625103, 21571107, and 21473121), Project 111 (Grant B12015), and the SFC of Tianjin (Grant 15JCZDJC37700).

REFERENCES

(1) Li, B.; Wen, H. M.; Cui, Y.; Qian, G.; Chen, B. Multifunctional lanthanide coordination polymers. *Prog. Polym. Sci.* **2015**, *48*, 40−84.
(2) (a) Weng, D. F.; Wang, Z. M.; Gao, S. Framework-structured weak ferromagnets. *Chem. Soc. Rev.* **2011**, *40*, 3157−3181. (b) Chang, L. X.; Xiong, G.; Wang, L.; Cheng, P.; Zhao, B. A 24-Gd nanocapsule with a large magnetocaloric effect. *Chem. Commun.* **2013**, *49*, 1055−1057. (c) Rinehart, J. D.; Long, J. R. Exploiting single-ion anisotropy in the design of f-element single-molecule magnets. *Chem. Sci.* **2011**, *2*, 2078−2085. (d) Roy, S.; Chakraborty, A.; Maji, T. K. Lanthanide−organic frameworks for gas storage and as magneto-luminescent materials. *Coord. Chem. Rev.* **2014**, *273−274*, 139−164. (e) Shi, P. F.; Zheng, Y. Z.; Zhao, X. Q.; Xiong, G.; Zhao, B.; Wan, F. F.; Cheng, P. 3 D MOFs containing trigonal bipyramidal Ln_5 clusters as nodes: large magnetocaloric effect and slow magnetic relaxation behavior. *Chem. - Eur. J.* **2012**, *18*, 15086−15091. (f) Zhang, P.; Zhang, L.; Wang, C.;

DOI: 10.1021/acs.inorgchem.7b00323
Inorg. Chem. XXXX, XXX, XXX−XXX

Xue, S.; Lin, S. Y.; Tang, J. Equatorially coordinated lanthanide single ion magnets. *J. Am. Chem. Soc.* **2014**, *136*, 4484−4487.

(3) (a) Cui, Y.; Song, R.; Yu, J.; Liu, M.; Wang, Z.; Wu, C.; Yang, Y.; Wang, Z.; Chen, B.; Qian, G. Dual-emitting MOF supersetdye composite for ratiometric temperature sensing. *Adv. Mater.* **2015**, *27*, 1420−1425. (b) He, Y.; Furukawa, H.; Wu, C.; O'Keeffe, M.; Krishna, R.; Chen, B. Low-energy regeneration and high productivity in a lanthanide-hexacarboxylate framework for high-pressure CO_2-CH_4-H_2 separation. *Chem. Commun.* **2013**, *49*, 6773−6775. (c) Hu, Z.; Deibert, B. J.; Li, J. Luminescent metal-organic frameworks for chemical sensing and explosive detection. *Chem. Soc. Rev.* **2014**, *43*, 5815−5840. (d) Liu, Y.; Pan, M.; Yang, Q. Y.; Fu, L.; Li, K.; Wei, S. C.; Su, C. Y. Dual-Emission from a Single-Phase Eu−Ag Metal−Organic Framework: An Alternative Way to Get White-Light Phosphor. *Chem. Mater.* **2012**, *24*, 1954−1960. (e) Rocha, J.; Carlos, L. D.; Paz, F. A.; Ananias, D. Luminescent multifunctional lanthanides-based metal-organic frameworks. *Chem. Soc. Rev.* **2011**, *40*, 926−940.

(4) (a) Liu, W. S.; Jiao, T. O.; Li, Y. Z.; Liu, Q. Z.; Tan, M. Y.; Wang, H.; Wang, L. F. Lanthanide Coordination Polymers and Their Ag^+-Modulated Fluorescence. *J. Am. Chem. Soc.* **2004**, *126*, 2280−2281. (b) Liu, B.; Wu, W. P.; Hou, L.; Wang, Y. Y. Four Uncommon Nanocage-based Ln-MOFs: Highly Selective Luminescent Sensing for Cu^{2+} ions and Selective CO_2 Capture. *Chem. Commun.* **2014**, *50*, 8731−8734. (c) Xu, H.; Hu, H. C.; Cao, C. S.; Zhao, B. Lanthanide Organic Frameworks as a Regenerable Luminescent Probe for Fe^{3+}. *Inorg. Chem.* **2015**, *54*, 4585−4587.

(5) (a) Han, J. W.; Hill, C. L. A Coordination Network That Catalyzes O2-Based Oxidations. *J. Am. Chem. Soc.* **2007**, *129*, 15094−15095. (b) Gándara, F.; Puebla, E. G.; Iglesias, M.; Proserpio, D. M.; Snejko, N.; Monge, M. A. Controlling the Structure of Arenedisulfonates toward Catalytically Active Materials. *Chem. Mater.* **2009**, *21*, 655−661. (c) Qin, J.; Wang, P.; Li, Q. Y.; Zhang, Y.; Yuan, D.; Yao, Y. M. Catalytic production of cyclic carbonates mediated by lanthanide phenolates under mild conditions. *Chem. Commun.* **2014**, *50*, 10952−10955. (d) Decortes, A.; Castilla, A. M.; Kleij, A. W. Salen-complex-mediated formation of cyclic carbonates by cycloaddition of CO_2 to epoxides. *Angew. Chem., Int. Ed.* **2010**, *49*, 9822−9837. (e) Guo, X.; Zhu, G.; Li, Z.; Sun, F.; Yang, Z.; Qiu, S. A lanthanide metal-organic framework with high thermal stability and available Lewis-acid metal sites. *Chem. Commun.* **2006**, 3172−3174. (f) Whiteoak, C. J.; Kielland, N.; Laserna, V.; Escudero-Adan, E. C.; Martin, E.; Kleij, A. W. A powerful aluminum catalyst for the synthesis of highly functional organic carbonates. *J. Am. Chem. Soc.* **2013**, *135*, 1228−1231. (g) Gong, Y. N.; Ouyang, T.; He, C. T.; Lu, T. B. Photoinduced water oxidation by an organic ligand incorporated into the framework of a stable metal-organic framework. *Chem. Sci.* **2016**, *7*, 1070−1075.

(6) (a) Xu, H.; Cao, C. S.; Zhao, B. A water-stable lanthanide-organic framework as a recyclable luminescent probe for detecting pollutant phosphorus anions. *Chem. Commun.* **2015**, *51*, 10280−10283. (b) Chen, B. L.; Wang, L. B.; Zapata, F.; Qian, G. D.; Lobkovsky, E. B. A Luminescent Microporous Metal-Organic Framework for the Recognition and Sensing of Anions. *J. Am. Chem. Soc.* **2008**, *130*, 6718−6719. (c) Duan, T. W.; Yan, B.; Weng, H. Europium activated yttrium hybrid microporous system for luminescent sensing toxic anion of Cr(VI) species. *Microporous Mesoporous Mater.* **2015**, *217*, 196−202. (d) Li, G. P.; Liu, G.; Li, Y. Z.; Hou, L.; Wang, Y. Y.; Zhu, Z. H. Uncommon pyrazoyl-carboxyl bifunctional ligand-based microporous lanthanide systems: sorption and luminescent sensing properties. *Inorg. Chem.* **2016**, *55*, 3952−3959.

(7) (a) Zhao, B.; Chen, X. Y.; Cheng, P.; Liao, D. Z.; Yan, S. P.; Jiang, Z. H. Coordination Polymers Containing 1D Channels as Selective Luminescent Probes. *J. Am. Chem. Soc.* **2004**, *126*, 15394−15395. (b) Chen, B.; Wang, L.; Xiao, Y.; Fronczek, F. R.; Xue, M.; Cui, Y.; Qian, G. A luminescent metal-organic framework with Lewis basic pyridyl sites for the sensing of metal ions. *Angew. Chem., Int. Ed.* **2009**, *48*, 500−503. (c) Zhao, X. Q.; Zhao, B.; Shi, W.; Cheng, P. Structures and luminescent properties of a series of Ln−Ag heterometallic coordination polymers. *CrystEngComm* **2009**, *11*, 1261−1269.

(8) (a) Dong, X. Y.; Wang, R.; Wang, J. Z.; Zang, S. Q.; Mak, T. C. W. Highly selective Fe^{3+} sensing and proton conduction in a water-stable sulfonate−carboxylate Tb−organic-framework. *J. Mater. Chem. A* **2015**, *3*, 641−647. (b) Chen, B.; Yang, Y.; Zapata, F.; Lin, G.; Qian, G.; Lobkovsky, E. B. Luminescent Open Metal Sites within a Metal−Organic Framework for Sensing Small Molecules. *Adv. Mater.* **2007**, *19*, 1693−1696.

(9) (a) Levina, A.; Lay, P. A. Mechanistic studies of relevance to the biological activities of chromium. *Coord. Chem. Rev.* **2005**, *249*, 281−298. (b) Wen, G. X.; Han, M. L.; Wu, X. Q.; Wu, Y. P.; Dong, W. W.; Zhao, J.; Li, D. S.; Ma, L. F. A multi-responsive luminescent sensor based on a super-stable sandwich-type terbium(III)-organic framework. *Dalton Trans.* **2016**, *45*, 15492−15499. (c) Liu, W.; Huang, X.; Xu, C.; Chen, C. Y.; Yang, L. Z.; Dou, W.; Chen, W. M.; Yang, H.; Liu, W. S. A multi-responsive regenerable europium-organic framework luminescent sensor for Fe^{3+}, Cr^{VI} anions, and picric acid. *Chem. - Eur. J.* **2016**, *22*, 18634. (d) Cao, C. S.; Hu, H. C.; Xu, H.; Qiao, W. Z.; Zhao, B. Two solvent-stable MOFs as a recyclable luminescent probe for detecting dichromate or chromate anions. *CrystEngComm* **2016**, *18*, 4445−4451.

(10) (a) Fei, H.; Bresler, M. R.; Oliver, S. R. A new paradigm for anion trapping in high capacity and selectivity: crystal-to-crystal transformation of cationic materials. *J. Am. Chem. Soc.* **2011**, *133*, 11110−11113. (b) Fei, H.; Han, C. S.; Robins, J. C.; Oliver, S. R. J. A Cationic Metal−Organic Solid Solution Based on Co(II) and Zn(II) for Chromate Trapping. *Chem. Mater.* **2013**, *25*, 647−652. (c) Fu, H.-R.; Xu, Z.-X.; Zhang, J. Water-Stable Metal−Organic Frameworks for Fast and High Dichromate Trapping via Single-Crystal-to-Single-Crystal Ion Exchange. *Chem. Mater.* **2015**, *27*, 205−210. (d) Lalonde, M.; Bury, W.; Karagiaridi, O.; Brown, Z.; Hupp, J. T.; Farha, O. K. Transmetalation: routes to metal exchange within metal−organic frameworks. *J. Mater. Chem. A* **2013**, *1*, 5453. (e) Wawrzkiewicz, M. Removal of C.I. Basic Blue 3 dye by sorption onto cation exchange resin, functionalized and non-functionalized polymeric sorbents from aqueous solutions and wastewaters. *Chem. Eng. J.* **2013**, *217*, 414−425. (f) Boyer, T. H.; Singer, P. C. Stoichiometry of Removal of Natural Organic Matter by Ion Exchange. *Environ. Sci. Technol.* **2008**, *42*, 608−613.

(11) Chakravarti, A. K.; Chowdhury, S. B.; Chakrabarty, S.; Chakrabarty, T.; Mukherjee, D. C. Liquid membrane multiple emulsion process of chromium(VI) separation from waste waters. *Colloids Surf., A* **1995**, *103*, 59−71.

(12) Shaham-Waldmann, N.; Paz, Y. Beyond charge separation: The effect of coupling between titanium dioxide and CNTs on the adsorption and photocatalytic reduction of Cr(VI). *Chem. Eng. J.* **2013**, *231*, 49−58.

(13) (a) Blaney, L. M.; Cinar, S.; SenGupta, A. K. Hybrid anion exchanger for trace phosphate removal from water and wastewater. *Water Res.* **2007**, *41*, 1603−1613. (b) Prasanna, S. V.; Vishnu Kamath, P. Chromate uptake characteristics of the pristine layered double hydroxides of Mg with Al. *Solid State Sci.* **2008**, *10*, 260−266.

(14) Sakakura, T.; Choi, J. C.; Yasuda, H. Transformation of Carbon Dioxide. *Chem. Rev.* **2007**, *107*, 2365−2387.

(15) (a) Wang, J. Y.; Huang, L.; Yang, R. Y.; Zhang, Z.; Wu, J. W.; Gao, Y. S.; Wang, Q.; O'Hare, D.; Zhong, Z. Y. Recent advances in solid sorbents for CO_2 capture and new development trends. *Energy Environ. Sci.* **2014**, *7*, 3478−3518. (b) Keith, D. W. Why Capture CO_2 from the Atmosphere. *Science* **2009**, *325*, 1654−1655. (c) Aresta, M.; Dibenedetto, A.; Angelini, A. Catalysis for the valorization of exhaust carbon: from CO_2 to chemicals, materials, and fuels. technological use of CO_2. *Chem. Rev.* **2014**, *114*, 1709−1742. (d) Jiang, H. L.; Tsumori, N.; Xu, Q. A series of (6,6)-connected porous lanthanide-organic framework enantiomers with high thermostability and exposed metal sites: scalable syntheses, structures, and sorption properties. *Inorg. Chem.* **2010**, *49*, 10001−10006. (e) Markewitz, P.; Kuckshinrichs, W.; Leitner, W.; Linssen, J.; Zapp, P.; Bongartz, R.; Schreiber, A.; Müller, T. E. Worldwide innovations in the development of carbon capture technologies and the utilization of CO2. *Energy Environ. Sci.* **2012**, *5*, 7281−7305. (f) Sumida, K.; Rogow, D. L.; Mason, J. A.; McDonald, T.

DOI: 10.1021/acs.inorgchem.7b00323
Inorg. Chem. XXXX, XXX, XXX−XXX

M.; Bloch, E. D.; Herm, Z. R.; Bae, T. H.; Long, J. R. Carbon dioxide capture in metal-organic frameworks. *Chem. Rev.* **2012**, *112*, 724−781.

(16) (a) Yoshida, M.; Ihara, M. Novel methodologies for the synthesis of cyclic carbonates. *Chem. - Eur. J.* **2004**, *10*, 2886−2893. (b) Li, P. Z.; Wang, X. J.; Liu, J.; Lim, J. S.; Zou, R. Q.; Zhao, Y. L. A triazole-containing metal-organic frameworks as a highly effective and substrate size-dependent catalyst for CO_2 conversion. *J. Am. Chem. Soc.* **2016**, *138*, 2142−2145.

(17) Zhao, Y.; Tian, J. S.; Qi, X. H.; Han, Z. N.; Zhuang, Y. Y.; He, L. N. Quaternary ammonium salt-functionalized chitosan: An easily recyclable catalyst for efficient synthesis of cyclic carbonates from epoxides and carbon dioxide. *J. Mol. Catal. A: Chem.* **2007**, *271*, 284−289.

(18) (a) Zheng, Q. X.; Morimoto, M.; Takanohashi, T. A novel process for the production of aromatic hydrocarbons from brown coal in water medium by hydrothermal oxidation and catalytic hydrothermal decarboxylation. *Fuel* **2016**, *182*, 437−445. (b) Bernard, A. M.; Cerioni, G.; Piras, P. P. Mechanism of decarbalkoxylation of arylmethylenepropanedioic acid dimethyl esters. *Tetrahedron* **1990**, *46*, 3929−3940. (c) Krapcho, A. P.; Ciganek, E. The krapcho dealkoxycarbonylation reaction of esters with a-electron-withdrawing substituents. *Organic Reactions* **2013**, *81*, 1−536.

(19) (a) Cui, Y.; Xu, H.; Yue, Y.; Guo, Z.; Yu, J.; Chen, Z.; Gao, J.; Yang, Y.; Qian, G.; Chen, B. A luminescent mixed-lanthanide metal-organic framework thermometer. *J. Am. Chem. Soc.* **2012**, *134*, 3979−3982. (b) Zhao, J.; Wang, Y. N.; Dong, W. W.; Wu, Y. P.; Li, D. S.; Zhang, Q. C. A Robust Luminescent Tb(III)-MOF with Lewis Basic Pyridyl Sites for the Highly Sensitive Detection of Metal Ions and Small Molecules. *Inorg. Chem.* **2016**, *55*, 3265−3271. (c) Lu, W. G.; Jiang, L.; Feng, X. L.; Lu, T. B. Three-dimensional lanthanide anionic metal-organic frameworks with tunable luminescent properties induced by cation exchange. *Inorg. Chem.* **2009**, *48*, 6997−6999. (d) Gong, Y. N.; Jiang, L.; Lu, T. B. A highly stable dynamic fluorescent metal-organic framework for selective sensing of nitroaromatic explosives. *Chem. Commun.* **2013**, *49*, 11113−11115.

(20) (a) Keizer, J. Nonlinear fluorescence quenching and the origin of positive curvature in stern-volmer plots. *J. Am. Chem. Soc.* **1983**, *105*, 1494−1498. (b) Lakos, Z.; Szarka, A.; Koszorus, L.; Somogyi, B. Quenching-resolved emission anisotropy: a steady state fluorescence method to study protein dynamics. *J. Photochem. Photobiol., B* **1995**, *27*, 55−60. (c) Kent, C. A.; Liu, D.; Meyer, T. J.; Lin, W. B. Amplified luminescence quenching of phosphorescent metal-organic frameworks. *J. Am. Chem. Soc.* **2012**, *134*, 3991−3994. (d) Zheng, M.; Tan, H. Q.; Xie, Z. Q.; Zhang, L. G.; Jing, X. B.; Sun, Z. C. Fast response and high sensitivity europium metal organic framework fluorescent probe with chelating terpyridine sites for Fe^{3+}. *ACS Appl. Mater. Interfaces* **2013**, *5*, 1078−1083.

(21) (a) Valyaev, D. A.; Lavigne, G.; Lugan, N. Manganese organometallic compounds in homogeneous catalysis: Past, present, and prospects. *Coord. Chem. Rev.* **2016**, *308*, 191−235. (b) Sampson, M. D.; Kubiak, C. P. Manganese Electrocatalysts with Bulky Bipyridine Ligands: Utilizing Lewis Acids To Promote Carbon Dioxide Reduction at Low Overpotentials. *J. Am. Chem. Soc.* **2016**, *138*, 1386−1393.

DOI: 10.1021/acs.inorgchem.7b00323
Inorg. Chem. XXXX, XXX, XXX−XXX